RESEARCH ARTICLE

Ordered Kinetochore Assembly in the Human-Pathogenic Basidiomycetous Yeast *Cryptococcus neoformans*

Lukasz Kozubowski,[a,b] Vikas Yadav,[c] Gautam Chatterjee,[c] Shreyas Sridhar,[c] Masashi Yamaguchi,[d] Susumu Kawamoto,[d] Indrani Bose,[e] Joseph Heitman,[b] Kaustuv Sanyal[c]

Division of Infectious Diseases, Department of Medicine, Duke University Medical Center, Durham, North Carolina, USA[a]; Department of Molecular Genetics and Microbiology, Duke University Medical Center, Durham, North Carolina, USA[b]; Molecular Mycology Laboratory, Molecular Biology and Genetics Unit, Jawaharlal Nehru Centre for Advanced Scientific Research, Bangalore, India[c]; Medical Mycology Research Center, Chiba University, Chiba, Japan[d]; Department of Biology, Western Carolina University, Cullowhee, North Carolina, USA[e]

L.K. and V.Y. contributed equally to this work

ABSTRACT **Kinetochores facilitate interaction between chromosomes and the spindle apparatus. The formation of a metazoan trilayered kinetochore is an ordered event in which inner, middle, and outer layers assemble during disassembly of the nuclear envelope during mitosis. The existence of a similar strong correlation between kinetochore assembly and nuclear envelope breakdown in unicellular eukaryotes is unclear. Studies in the hemiascomycetous budding yeasts *Saccharomyces cerevisiae* and *Candida albicans* suggest that an ordered kinetochore assembly may not be evolutionarily conserved. Here, we utilized high-resolution time-lapse microscopy to analyze the localization patterns of a series of putative kinetochore proteins in the basidiomycetous budding yeast *Cryptococcus neoformans*, a human pathogen. Strikingly, similar to most metazoa but atypical of yeasts, the centromeres are not clustered but positioned adjacent to the nuclear envelope in premitotic *C. neoformans* cells. The centromeres gradually coalesce to a single cluster as cells progress toward mitosis. The mitotic clustering of centromeres seems to be dependent on the integrity of the mitotic spindle. To study the dynamics of the nuclear envelope, we followed the localization of two marker proteins, Ndc1 and Nup107. Fluorescence microscopy of the nuclear envelope and components of the kinetochore, along with ultrastructure analysis by transmission electron microscopy, reveal that in *C. neoformans*, the kinetochore assembles in an ordered manner prior to mitosis in concert with a partial opening of the nuclear envelope. Taken together, the results of this study demonstrate that kinetochore dynamics in *C. neoformans* is reminiscent of that of metazoans and shed new light on the evolution of mitosis in eukaryotes.**

IMPORTANCE **Successful propagation of genetic material in progeny is essential for the survival of any organism. A proper kinetochore-microtubule interaction is crucial for high-fidelity chromosome segregation. An error in this process can lead to loss or gain of chromosomes, a common feature of most solid cancers. Several proteins assemble on centromere DNA to form a kinetochore. However, significant differences in the process of kinetochore assembly exist between unicellular yeasts and multicellular metaozoa. Here, we examined the key events that lead to formation of a proper kinetochore in a basidiomycetous budding yeast, *Cryptococcus neoformans*. We found that, during the progression of the cell cycle, nonclustered centromeres gradually clustered and kinetochores assembled in an ordered manner concomitant with partial opening of the nuclear envelope in this organism. These events have higher similarity to mitotic events of metazoans than to those previously described in other yeasts.**

Received 2 August 2013 **Accepted** 11 September 2013 **Published** 1 October 2013

Citation Kozubowski L, Yadav V, Chatterjee G, Sridhar S, Yamaguchi M, Kawamoto S, Bose I, Heitman J, Sanyal K. 2013. Ordered kinetochore assembly in the human-pathogenic basidiomycetous yeast *Cryptococcus neoformans*. mBio 4(5):e00614-13. doi:10.1128/mBio.00614-13.

Editor Judith Berman, University of Minnesota, GCD

Address correspondence to Kaustuv Sanyal, sanyal@jncasr.ac.in, and Lukasz Kozubowski, lukasz.kozubowski@duke.edu/lkozubo@clemson.edu.

High-fidelity chromosome segregation is essential for faithful propagation of genetic information. The process of chromosome segregation is powered by the dynamic interaction between the chromosomes and the spindle microtubules. The chromosomal attachment site of spindle microtubules is a multimeric proteinaceous structure formed on the centromere DNA, termed the kinetochore (KT) (1). An error in the KT-microtubule interaction can result in improper chromosome segregation, leading to aneuploidy, a hallmark of several cancers (2, 3).

While the trilaminar architecture of the KT is conserved from yeast to humans, structural and functional evolution of some of the KT proteins is evident (4). Among the three layers of the KT, the components of the inner layer that interact directly with DNA are conserved in organisms with regional centromeres (centromere DNA is >3 kb in length) (5). The centromere-specific histone H3 of the CENP-A/Cse4 family and CENP-C/Mif2 are two such evolutionarily conserved inner KT proteins (6). Several middle KT proteins, such as Mis12/Mtw1 and Nuf2, are present in most

eukaryotes. In contrast, the 10-subunit outer KT Dam1 protein complex is found only in fungi (7–9).

Though the overall architecture of the KT is largely conserved, its assembly and regulation vary among species. Most metazoans undergo open mitosis. Ordered KT assembly is orchestrated with disassembly of the nuclear envelope (NE) in open mitosis, where the middle and outer KT assemble on the constitutive inner KT to allow access of microtubules to the centromere (10–12). Current knowledge about the dynamics of the fungal KT is primarily based on studies involving three model ascomycete species (6), the budding yeasts *Saccharomyces cerevisiae* and *Candida albicans* and the fission yeast *Schizosaccharomyces pombe*. Both budding yeasts undergo closed mitosis, as the NE never breaks down (13, 14) and the KT is fully assembled and attached to microtubules throughout the cell cycle (15). In contrast, in the fission yeast *S. pombe*, most proteins of the outer KT assemble only during mitosis, although the NE remains intact (16, 17).

Cryptococcus neoformans is a human pathogen known to cause meningitis primarily in immunocompromised but also in immunocompetent patients (18). *C. neoformans* has an 18.9-Mb genome distributed in 14 nuclear chromosomes and one 21-kb mitochondrial chromosome (19). By localizing several KT proteins, microtubules, and NE markers, we demonstrate, for the first time, that a metazoanlike ordered process of KT assembly exists in a fungal species. Our results suggest that mitotic events associated with metazoans—ordered KT assembly, interaction between KTs and microtubules only during mitosis, and opening of the NE—have evolved in fungal species.

RESULTS AND DISCUSSION

To study the dynamics of KT assembly in *C. neoformans*, we identified and fluorescently tagged proteins with homology to eukaryotic KT subunits that represent the three functional layers (Fig. 1A; see Table S1 in the supplemental material), as follows: CENP-A/Cse4 and CENP-C/Mif2 (inner KT components), Mis12/Mtw1 and Nuf2 (middle KT proteins), and Dad1 and Dad2, two constituents of the Dam1 complex (an outer KT-protein complex). Strains expressing the tagged proteins showed no obvious growth defects. In cells undergoing mitosis, each of these six fluorescently tagged proteins exhibited localization typical of a budding yeast KT protein, suggesting that each of these six putative KT protein homologs in *C. neoformans* is indeed localized at the KT (Fig. 1B).

***C. neoformans* centromeres are not clustered in nondividing cells.** In *C. neoformans*, similar to other basidiomycetous yeasts, nuclear division occurs within the daughter cell (20–23). To visualize the dynamics and changes associated with chromatin, we followed the localization of green fluorescent protein-tagged histone H4 (GFP-H4) (Fig. 1C). Consistent with previous reports, GFP-H4 transitioned entirely into the daughter cell to undergo division. In the daughter cell, the surface area of the GFP-H4 signal was reduced by ~66% compared to the signal before the nuclear mass migrated through the mother bud neck, suggesting significant chromatin condensation during mitosis. Notably, at this stage, GFP-H4 appeared as a doublet (Fig. 1C, arrow). Subsequently, the nuclear division occurred in the daughter cell; half of the nuclear mass migrated back into the mother cell, and the other half remained in the daughter cell.

We next examined the dynamics of KTs by performing time-lapse imaging of cells expressing fluorescently tagged CENP-A, mCherry-Cse4. To better discern stages of the cell cycle, the spindle was visualized with GFP-tagged α-tubulin (GFP-tubulin). In striking contrast to hemiascomycetous budding yeasts (*S. cerevisiae* and *C. albicans*), in which KTs are always clustered (9, 14, 24–27), mCherry-Cse4 showed multiple distinct dots in nondividing cells, including unbudded cells and cells with small buds (budding index less than or equal to ~0.4) (Fig. 1D; see Fig. S1A and B in the supplemental material). KTs are not usually clustered in most metazoans. Semiquantitative analysis of fluorescence intensity revealed that the number of mCherry-Cse4 dots was consistent with the number of centromeres (14 chromosomes per haploid cell) in *C. neoformans* (Fig. S1A). The circular arrangement of mCherry-Cse4 dotlike signals in most nondividing cells suggested localization adjacent to the nuclear periphery. Peripheral localization was further confirmed in cells that also expressed GFP-H4 or the NE marker protein GFP-Ndc1 (Fig. S1D and E). The number of dotlike signals of mCherry-Cse4 gradually decreased until, ultimately, in large budded cells (budding index of 0.4 to 0.55), the mCherry-Cse4 was visible as a single bright dot that subsequently migrated into the mother-bud neck (Fig. 1D; Fig. S1B). Interestingly, when clustering was nearly complete, mCherry-Cse4 appeared to contact a bundle of GFP-tubulin cables, suggesting that clustering of KTs and the attachment of microtubules to the KT occur concomitantly (Fig. 1D; Fig. S1A and B). Clustered mCherry-Cse4 was always at the NE, similar to hemiascomycetous budding yeasts (14, 24, 28, 29). In the daughter cell, a dotlike signal of GFP-tubulin underwent a transition into an elongated rod which was surrounded by 2 bars of mCherry-Cse4 when observed in a single focal plane (Fig. 1D, arrow; Fig. S1C). While the architecture of this microtubule KT arrangement remains to be determined, it may be functionally analogous to the metaphase plate of metazoans. At this stage, cytoplasmic microtubules were no longer visible. Within a minute or less after astral microtubules became visible, the mCherry-Cse4 signals divided into two separate dots, with one migrating back to the mother cell. After division of mCherry-Cse4, cytoplasmic microtubules reappeared and the mCherry-Cse4 began to decluster, forming dotlike signals similar to those observed in nondividing cells.

Microtubules are necessary for clustering of kinetochores prior to mitosis. The concomitant localization of KTs and tubulin when KTs were clustered prompted us to examine whether microtubules play a role in the clustering of KTs. To test this, we used nocodazole (Noc) to depolymerize microtubules in a strain that coexpressed mCherry-Cse4 (to assess the position of centromeres) and GFP-Ndc1 (to assess the state of the NE and the stage during the cell cycle) (Fig. 2A). First, we obtained a population of mostly unbudded cells (96% unbudded) by limiting oxygen during growth (30). In this starting population, mCherry-Cse4 was not clustered (Fig. 2A). Approximately 70 min after release from the arrest, both the control and Noc-treated cells were mostly budded, indicating resumption of synchronized growth and confirming that Noc treatment did not affect the establishment of cell polarity and the subsequent growth of the bud. While 47% of the control cells had the mCherry-Cse4 signal either in the daughter cell or divided between the mother and the daughter, no such cells were found in the Noc-treated sample at 70 min (Fig. 2B). As expected, a significant portion of the control cells (21%) showed clustered mCherry-Cse4. The average ratio of the bud/mother size in these cells was 0.6 (standard deviation [SD] = 0.09). Based on

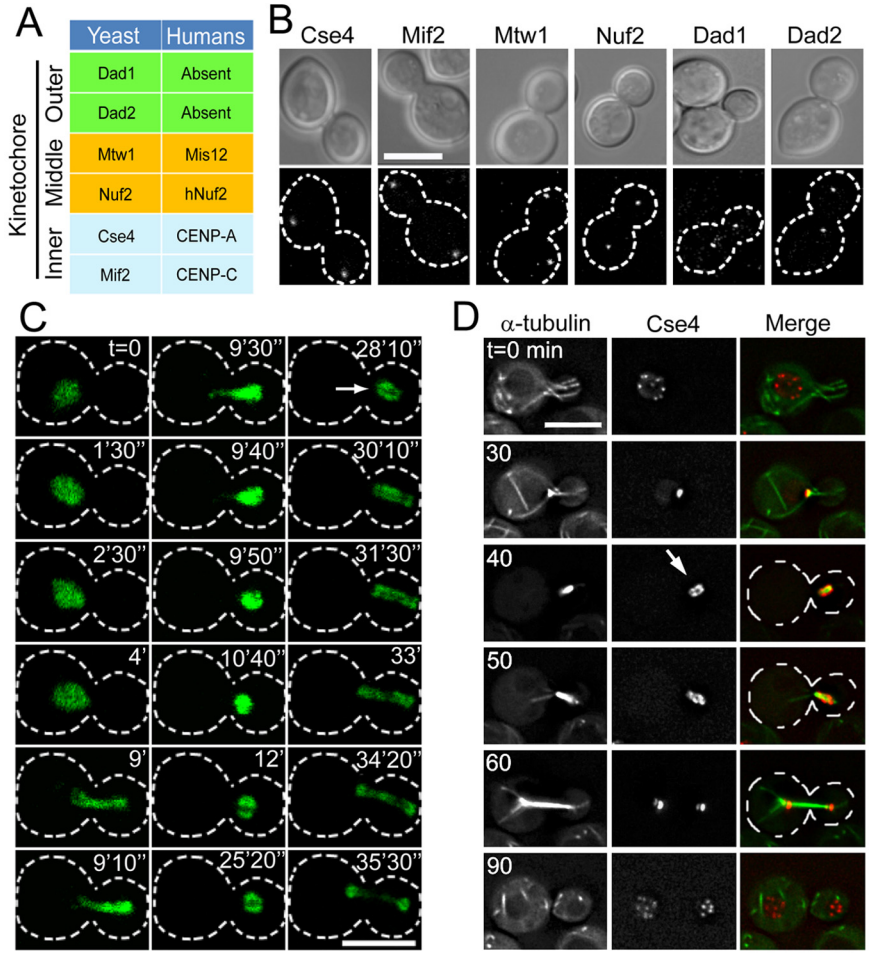

FIG 1 Nuclear division and dynamics of centromeres during cell cycle in *C. neoformans*. (A) Conserved proteins representing three layers of a fungal kinetochore that were chosen for the analysis. (B) In cells undergoing mitosis, putative kinetochore proteins tagged with mCherry (Cse4 [strain CNV101], Mif2 [strain CNV102], and Mtw1 [strain CNV103]) or GFP (Nuf2 [strain SHR515], Dad1 [strain CNV104], and Dad2 [strain SHR107]) show localization similar to that of the kinetochore in ascomycetous budding yeasts. (C) Cells expressing a chromatin marker, GFP-histone H4 (strain CNV108), were analyzed by time-lapse microscopy. During mitosis, the chromatin first moves entirely to the daughter cell and then condenses and forms a doubletlike structure (arrow). Finally, the chromatin divides into two compact signals between the daughter and mother cell. (D) Cells expressing GFP-tubulin and the inner kinetochore marker mCherry-Cse4 (strain LK275) were studied by time-lapse Z-section microscopy, and single focal planes are shown. Initially nonclustered mCherry-Cse4 converges into a single dot in the mother cell. In the daughter cell, mCherry-Cse4 rearranges into a doublet that surrounds a single rod of GFP-tubulin, a putative spindle ($t = 40$, arrow). At this stage, cytoplasmic GFP-tubulin cables are no longer visible. After mCherry-Cse4 divides between the daughter and mother cells, mCherry-Cse4 declusters and the GFP-tubulin cytoplasmic cables reappear ($t = 90$). See also Fig. S1 in the supplemental material. Bars, 5 μm.

this information, we examined Noc-treated cells with a bud/mother size ratio of ≥0.62 for clustering of mCherry-Cse4. Strikingly, we found that 39% of all Noc-treated cells had an average bud/mother size ratio of 0.72 (SD = 0.09) and nonclustered mCherry-Cse4 in the mother with no signal in the daughter. No Noc-treated cells with clustered mCherry-Cse4 signals were found at 70 min except for a small percentage (9%) of cells with aberrant localization of GFP-Ndc1. In these cells, chromatin was significantly compacted (data not shown) and GFP-Ndc1 formed a tight ring surrounding a small cluster of mCherry-Cse4 and/or formed a bright cluster away from mCherry-Cse4 (Fig. 2A). We hypothesize that, in these cells, a process of chromatin condensation bypassed the requirement for microtubules without hindering the formation of the trilayered KT structure and resulted in bringing centromeres in close proximity. In summary, our findings suggest that microtubules are involved in the clustering of centromeres prior to mitosis in *C. neoformans*. Clustering of KTs in *S. cerevisiae* during mitosis depends on the kinesin-8 homologue Kip3, while during interphase, it requires both microtubules and the KT-associated protein Slk19 (31, 32). Since the sequence homolog of Kip3 in *C. neoformans* remains uncharacterized and there is no obvious homologue of Slk19, the precise contribution of microtubules to clustering of centromeres will require further studies.

Kinetochores in *C. neoformans* assemble in an ordered manner. The appearance of nonclustered centromeres in *C. neoformans* suggests a fundamental difference in centromere dynamics between *C. neoformans* and the ascomycetous budding yeasts where such studies have already been performed. This led us to analyze the localization dynamics of the KT proteins from all 3 KT layers in *C. neoformans*. An inner KT protein, Mif2-mCherry, showed persistent localization similar to that of GFP-Cse4, suggesting that the inner KT is constitutively present at the centro-

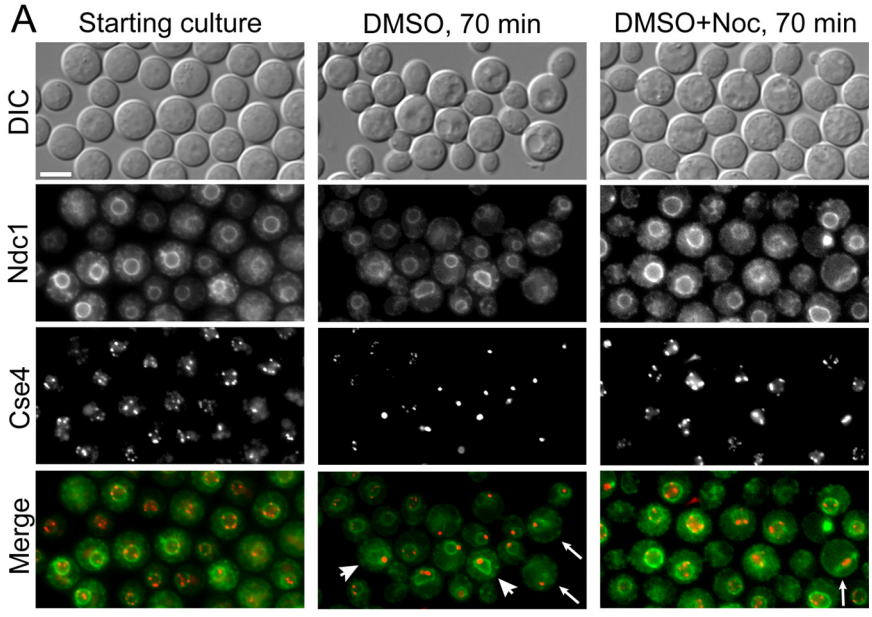

B

Time (min)	Sample	Budded	Cells in mitosis	Cse4 clustered cells not yet dividing	Cse4 declustered	
					Small-budded	Large-budded
0	Control	3	0	0	3	0
	Nocod.	1	0	0	1	0
50	Control	66	5	20	41	0
	Nocod.	71	0	4*	49	18
70	Control	81	47	21	12	0
	Nocod.	68	0	9*	18	39

Numbers represent % (at least 100 cells were counted in each category)
* In these cells Ndc1 was delocalized

FIG 2 Clustering of centromeres requires microtubules. (A) Cells expressing mCherry-Cse4 and GFP-Ndc1 (strain CNV111) were synchronized in G_1/G_2 and released from the arrest in the presence of nocodazole (1 μg/ml) or dimethyl sulfoxide (DMSO) as a control. At 70 min after the release, the majority of nocodazole-treated cells showed nonclustered mCherry-Cse4, while in the control sample, the majority of cells either showed clustered centromeres or progressed through mitosis. (B) Quantification of cells with respect to the stage of the cell cycle and percentage of centromere clustering. Bar, 5 μm.

mere (Fig. 3A and B). In contrast, the middle KT protein Mis12/Mtw1 and the outer KT protein Dad1 did not colocalize with inner KT proteins Cse4 and Mif2 in cells that showed nonclustered KTs (Fig. 3C and D). Thus, the middle and outer KT do not assemble at the stage when KTs are nonclustered. This possibility was further confirmed by using another set of proteins, the middle KT protein GFP-Nuf2 and an outer KT component, GFP-Dad2 (see Fig. S2A and B in the supplemental material). Based on these results, we conclude that the middle and outer KT layers form only during mitosis. The relative localization timing of the GFP-Dad1 and the Mtw1-mCherry in the same cells revealed that the GFP-Dad1 signals became visible later than the appearance of Mtw1-mCherry but disappeared before Mtw1-mCherry (Fig. 3E). An analysis of the budding index of the cells examined ($n = 100$) confirmed a difference in the timing of the appearance of middle KT (budding index equal to 0.4) and outer KT proteins (budding index equal to 0.55; $P = 0.0001$) (Fig. S2C). Taken together, these results indicate that the assembly of the KT in *C. neoformans* is an ordered process in which the inner KT remains assembled on the centromere DNA throughout the entire cell cycle and components of the middle KT are incorporated prior to mitosis, concomitant with KT clustering, followed by complete assembly of the KT just before KTs start moving to the daughter cell (Fig. 3F). This process has not been described in yeasts and is strikingly similar to the dynamics of KT assembly in metazoans. Thus, our study suggests evolutionary conservation of KT assembly from basidiomycete yeasts to humans.

The nuclear envelope opens partially during mitosis in *C. neoformans*. Ordered KT assembly and open mitosis where the NE breaks down are hallmarks of metazoan mitosis. Having established metazoanlike ordered assembly of the KT in *C. neoformans*, we sought to examine the status of the NE in this fungal pathogen. First, we followed the localization of the integral NE protein Ndc1 (33, 34). GFP-Ndc1 outlined the NE throughout the entire duration of nuclear division (Fig. 4A). Approximately half of the GFP-Ndc1 signal that outlined the NE remained in the mother cell, while clustered mCherry-Cse4 led the rest of the GFP-Ndc1-marked NE into the daughter cell at the onset of mitosis. In a closer look, the GFP-Ndc1 fluorescent signal immediately adjacent to the clustered mCherry-Cse4 appeared somewhat weaker

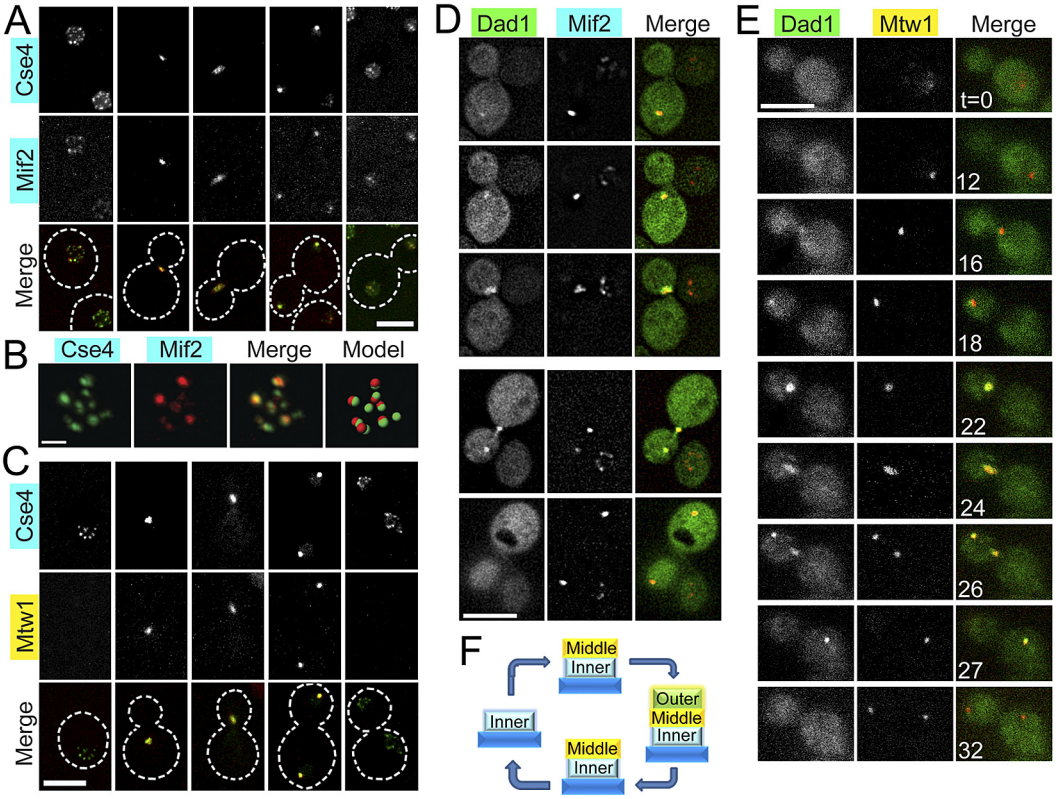

FIG 3 Ordered kinetochore assembly in *C. neoformans*. (A) Two inner kinetochore proteins, GFP-Cse4 and Mif2-mCherry (strain CNV115), colocalized at all stages of the cell cycle. Both proteins colocalized as separate dots in unbudded cells (first column), small-budded cells (not shown) and soon after cytokinesis (last column) but remained clustered during mitosis (middle three columns). (B) A 3-dimensional (3-D) reconstruction based on Z-stack images of an unbudded cell shows a complete overlap of GFP-Cse4 and Mif2-mCherry. (C) The middle kinetochore protein Mtw1-mCherry was not visible in cells where the inner kinetochore protein GFP-Cse4 was found as multiple nonclustered signals (strain CNV116; the first and the last columns). However, Mtw1-mCherry colocalized with clustered GFP-Cse4 (middle three columns). (D) The outer kinetochore component GFP-Dad1 became visible prior to mitosis when it colocalized with the inner kinetochore protein Mif2-mCherry in a single cluster (strain CNV118). (E) Colocalization of an outer (GFP-Dad1) and a middle (Mtw1-mCherry) kinetochore protein showed that GFP-Dad1 was loaded onto the kinetochore later than Mtw1-mCherry (strain CNV117). GFP-Dad1 was visible during mitosis (t = 16 to 27 min) and disappeared soon after chromosome segregation, while Mtw1-mCherry remained present (t = 32 min). (F) Schematic showing ordered assembly of kinetochore proteins. The inner, middle, and outer kinetochore protein names are highlighted in blue, yellow, and green, respectively. See also Fig. S2 in the supplemental material. Bars, 5 μm (A, C, D, and E) and 1 μm (B).

or discontinuous (Fig. 4B). These data suggest that the NE remains largely intact during mitosis in *C. neoformans* and only a partial opening of the NE takes place, specifically, near clustered KTs. Further analysis of the NE using transmission electron microscopy (TEM) revealed that, while the NE stayed largely intact during mitosis in *C. neoformans*, it did rupture at the point where the spindle broke through the NE during the migration of the spindle into the daughter cell (Fig. 4C; see Table S2 in the supplemental material). TEM indicated that the nucleolus was not present during mitosis (Table S2). This was confirmed with the strain expressing the nucleolar marker GFP-Nop1 (Fig. 4D, t = 20 min). We also followed the localization of the fluorescently tagged Nup107, an essential component of the nuclear pore complex (NPC) (35). Time lapse imaging of GFP-Nup107 and mCherry-Cse4 showed that the GFP-Nup107 signal disappeared during the stage when mCherry-Cse4 was present in the daughter cell (Fig. 4E). Based on these results, we propose that *C. neoformans* undergoes a semiopen mitosis characterized by a partial breakage of the NE near spindle pole bodies (SPBs) and complete disassembly of the NPC (Fig. 5A). Recently, various types of mitosis other than the conventional open or closed mitosis have been reported in fungi. A semiopen type of mitosis was described in *Aspergillus nidulans*, where some of the NPC proteins disassemble (36). Another type of mitosis was reported in the fission yeast *Schizosaccharomyces japonicus*, where the NE breaks during anaphase (37, 38). In *Ustilago maydis*, another basidiomycetous yeast, the NE breaks near SPBs and NPCs disassemble completely (22, 39). The type of mitosis in *C. neoformans* appears similar to that of *U. maydis*, with subtle differences in the dynamics of the NE. In *U. maydis*, the NE remains in the mother cell and does not enclose chromatin during mitosis, but in *C. neoformans*, a part of the NE moves to the daughter cell and encloses the DNA during division.

Taken together, the analysis of nuclear division in *C. neoformans* suggests that, in basidiomycetous budding yeasts, KTs assemble in an ordered manner in concert with partial disassembly of the NE (Fig. 5A). We propose that this form of mitosis was an ancestral mode present in basidiomycetes and the mitotic events in hemiascomycetous budding yeasts might have evolved independently (Fig. 5B). The intriguing nonclustered state of centromeres and the apparent localization near the NE in nondividing cells are reminiscent of the localization reported in some metazoan cells (40–43). As clustering of centromeres in *C. neoformans*

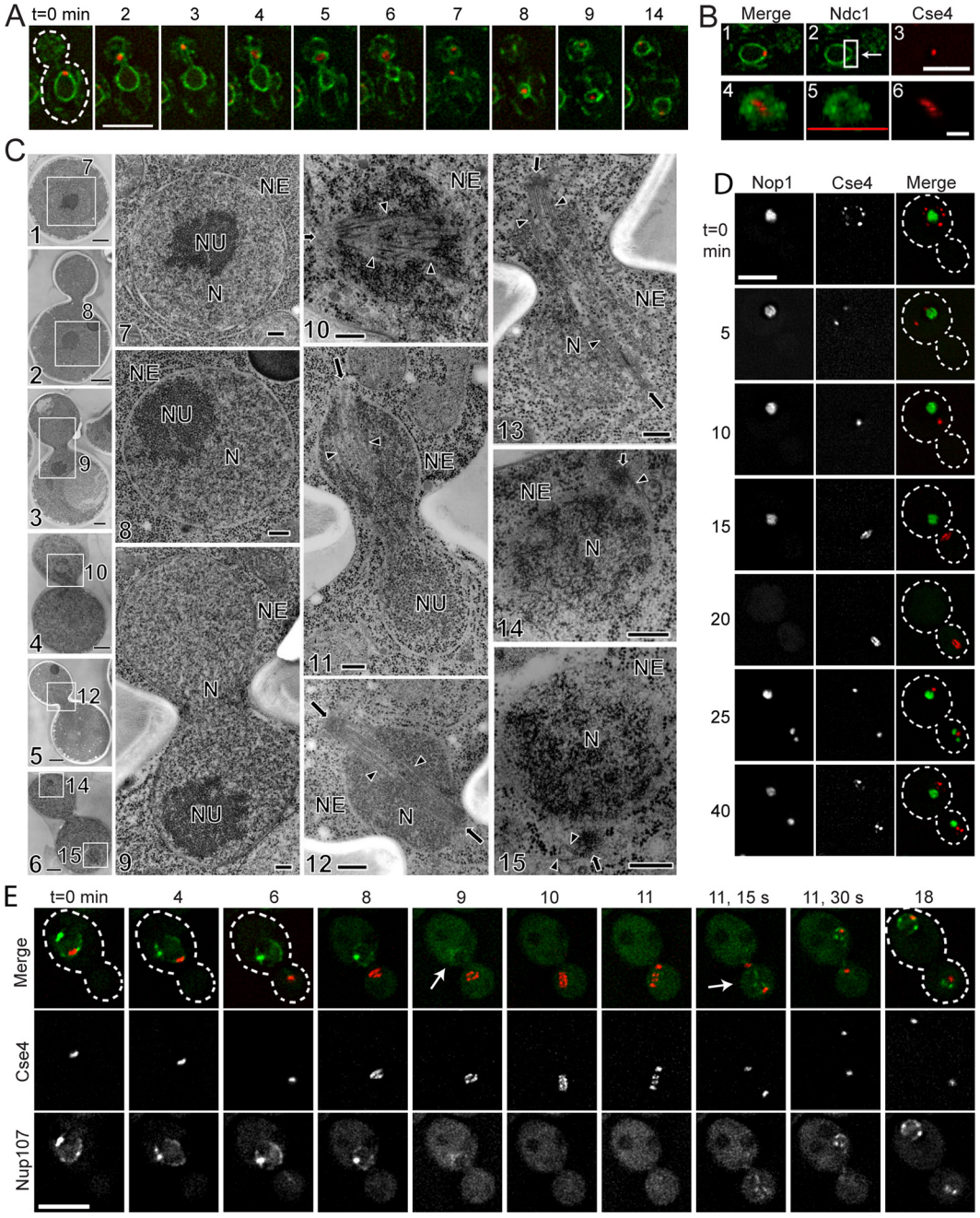

FIG 4 The nuclear envelope in *C. neoformans* breaks open partially during mitosis. (A) The nuclear membrane (visualized by GFP-Ndc1 in strain CNV111) was largely intact throughout the cell cycle. Clustered mCherry-Cse4 led an invagination of the nuclear membrane into the daughter cell at the onset of mitosis (t = 2 to 3 min) (B) A 3-D reconstruction of Z-stack images of a cell from panel A at $t = 0$ showed a discontinuous signal of GFP-Ndc1 at the site where mCherry-Cse4 was clustered, suggesting partial opening of the nuclear membrane near clustered kinetochores. Panels 4, 5, and 6 show projections of the area in panel 2 indicated with the arrow. The red line in panel 5 indicates the surface of the medium. (C) TEM analysis of mitosis in *C. neoformans*. In images 2 to 6, the daughter cell is the one on top (smaller than the mother cell). Images: 1 and 7, G_1-S phase; 2 and 8, G_2 phase; 3 and 9, prophase; 4, 10, and 11, prometaphase; 5 and 12, metaphase; 13, anaphase; 6, 14, and 15, telophase. Nuclear envelope (NE) was intact at G_1 through prophase, had broken near the spindle pole body (arrow) at prometaphase, and was closed at the end of telophase. Nucleolus (NU) was visible at G_1 through prophase, stayed in the mother cell at prometaphase, disappeared at metaphase, and reappeared after telophase. Spindle pole body resided on the nuclear envelope as one duplicated form at G_1 though G_2 phase, separated into two at prophase, entered the nuclear region by breaking the nuclear envelope at prometaphase, was located at the spindle poles at metaphase and anaphase, and was extruded back to the cytoplasm from the nuclear region at telophase. Microtubules (arrowheads) were distributed in the cytoplasm at G_1 through prophase and appeared in the nucleus (N) at prometaphase through middle of telophase. (D) Time lapse imaging with the nucleolus marker GFP-Nop1 showed that the nucleolus disappeared during mitosis when mCherry-Cse4 was present in the doublet stage (strain LK353). (E) Time-lapse analysis of nuclear pore protein GFP-Nup107 and mCherry-Cse4 (strain LK317). GFP-Nup107 was not present on the NE during metaphase (t = 9 to 11.15 min), suggesting that NPCs disassembled at this stage. After genomic division, GFP-Nup107 was again visible on the NE, marking the reassembly of NPCs after mitosis. Bars, 5 μm (A, B [top], D, and E), 1 μm (B [bottom] and C [1 to 6]), 250 nm (C [7 to 15]).

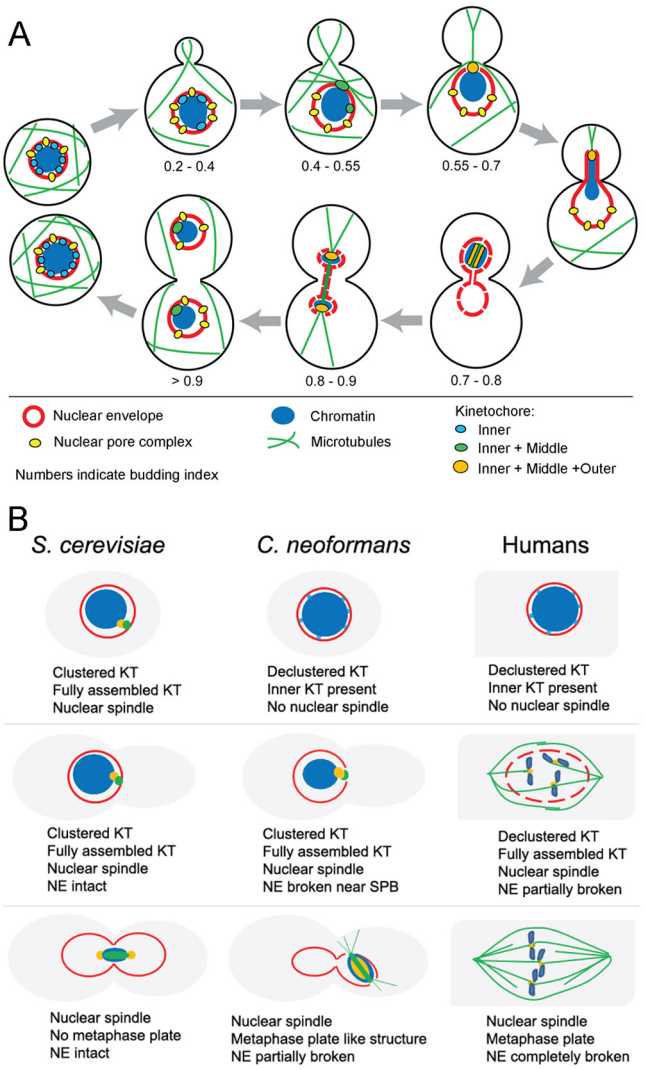

FIG 5 Key events during mitotic cell cycle in *C. neoformans*. (A) A model showing clustering of centromeres, a gradual change in kinetochore architecture, and the nuclear envelope dynamics during the progression of the cell cycle in *C. neoformans*. The budding index at each stage was calculated by measuring the relative bud sizes of at least 100 cells. (B) A comparison of key mitotic events in *S. cerevisiae*, *C. neoformans*, and humans.

appears to be completed before assembly of the outer KT, microtubule-mediated clustering of centromeres may not occur simply via the attachment of microtubules to the assembled KT. Further studies on mechanisms of KT clustering and their assembly in *C. neoformans* should lead to a better understanding of the evolution of mitosis in eukaryotes.

MATERIALS AND METHODS

Strains and plasmids. The strains and plasmids used in this study are listed in Table S3 in the supplemental material. *C. neoformans* culture was grown in yeast extract-peptone-dextrose (YPD) medium at 30°C.

Construction of fluorescently tagged proteins. Fluorescent fusion proteins were made by either cloning or overlap PCR. The list of primers used for construction is given in Table S4 in the supplemental material. Plasmids or overlap PCR products to express GFP and mCherry fusion proteins were mainly constructed using a method described previously (44) (See Text S1 in the supplemental material for detail).

Two rounds of transformation were used to tag the two different proteins in the same strain, and medium containing both nourseothricin (NAT) and G418 was used for selection. The transformants were screened by fluorescence microscopy.

Fluorescence microscopy. Cells were grown in the YPD medium for 14 to 16 h and pelleted at 4,000 rpm. The cells were then washed once with distilled water and finally resuspended in distilled water. The cells were placed on slides, covered with coverslips, and observed under a microscope. For live-cell imaging, an overnight YPD or synthetic complete medium-grown culture was diluted in fresh synthetic complete growth medium and grown for 3 h. Next, ~0.5 μl of cell suspension was placed on a slide containing a thin complete growth medium–2% agarose patch and covered with a coverslip. Images were captured at 100× using either a Carl Zeiss confocal laser scanning microscope (LSM 510 META) or the DeltaVision system (Olympus IX-71 base) equipped with a CoolSnap HQ2 high-resolution charge-coupled-device (CCD) camera and a 100× objective (100×/1.40 oil UPLSAPO100X0 1-U2B836 WD 120-μm differential interference contrast [DIC] ∞/0.17/FN26.5, UIS2 series). The filters used (Chroma) were GFP/fluorescein isothiocyanate (FITC) 475/28, mCherry/AF594 575/25 for excitation and GFP/FITC 525/50, mCherry/AF594 632/60 for emission and a Dual em pass GFP/mCherry filter for high-speed imaging. For more detailed description of the DeltaVision system, see http://microscopy.duke.edu/dv.html. For confocal microscopy, Ar 488 and HeNe 543 lasers were used for excitation of GFP and mCherry, respectively. The image processing was done using the Zeiss image-processing software LSM 5 Image Examiner or ImageJ, Image-Pro Plus, or Photoshop (Adobe Systems, San Jose, CA).

SUPPLEMENTAL MATERIAL

Supplemental material for this article may be found at http://mbio.asm.org/lookup/suppl/doi:10.1128/mBio.00614-13/-/DCSupplemental.

Text S1, PDF file, 0.4 MB.
Figure S1, PDF file, 0.6 MB.
Figure S2, PDF file, 0.5 MB.
Table S1, PDF file, 0.1 MB.
Table S2, PDF file, 0.1 MB.
Table S3, PDF file, 0.4 MB.
Table S4, PDF file, 0.1 MB.

ACKNOWLEDGMENTS

We thank Beth Sullivan for her comments on the manuscript. We thank B. Suma for confocal microscopy.

This work is supported by intramural funding of JNCASR to K.S. V.Y. is a JRF and G.C. is an SRF funded by CSIR, Government of India. I.B. was a visiting scientist supported by JNCASR. S.S. is supported by JNCASR. L.K. was supported by NIH/NIAID R37 grant AI39115-15 and R01 grant AI50113-10 to J.H. This study was partly supported by the Cooperative Research Program of the Medical Mycology Research Center, Chiba University, to M.Y. and S.K.

REFERENCES

1. **Sullivan BA, Blower MD, Karpen GH.** 2001. Determining centromere identity: cyclical stories and forking paths. Nat. Rev. Genet. **2:**584–596.
2. **Cimini D.** 2008. Merotelic kinetochore orientation, aneuploidy, and cancer. Biochim. Biophys. Acta **1786:**32–40.
3. **Holland AJ, Cleveland DW.** 2012. Losing balance: the origin and impact of aneuploidy in cancer. EMBO Rep. **13:**501–514.
4. **Meraldi P, McAinsh AD, Rheinbay E, Sorger PK.** 2006. Phylogenetic and structural analysis of centromeric DNA and kinetochore proteins. Genome Biol. **7:**R23. doi:10.1186/gb-2006-7-3-r23.
5. **Sanyal K.** 2012. How do microbial pathogens make *CENs*? PLoS Pathog. **8:**e1002463. doi:10.1371/journal.ppat.1002463.
6. **Roy B, Varshney N, Yadav V, Sanyal K.** 2013. The process of kinetochore assembly in yeasts. FEMS Microbiol. Lett. **338:**107–117.
7. **Lampert F, Westermann S.** 2011. A blueprint for kinetochores—new insights into the molecular mechanics of cell division. Nat. Rev. Mol. Cell Biol. **12:**407–412.

8. **Westermann S, Drubin DG, Barnes G.** 2007. Structures and functions of yeast kinetochore complexes. Annu. Rev. Biochem. **76:**563–591.
9. **Thakur J, Sanyal K.** 2011. The essentiality of the fungus-specific Dam1 complex is correlated with a one-kinetochore-one-microtubule interaction present throughout the cell cycle, independent of the nature of a centromere. Eukaryot. Cell **10:**1295–1305.
10. **Gascoigne KE, Cheeseman IM.** 2011. Kinetochore assembly: if you build it, they will come. Curr. Opin. Cell Biol. **23:**102–108.
11. **Güttinger S, Laurell E, Kutay U.** 2009. Orchestrating nuclear envelope disassembly and reassembly during mitosis. Nat. Rev. Mol. Cell Biol. **10:** 178–191.
12. **Gascoigne KE, Cheeseman IM.** 2013. CDK-dependent phosphorylation and nuclear exclusion coordinately control kinetochore assembly state. J. Cell Biol. **201:**23–32.
13. **De Souza CP, Osmani SA.** 2007. Mitosis, not just open or closed. Eukaryot. Cell **6:**1521–1527.
14. **Thakur J, Sanyal K.** 2012. A coordinated interdependent protein circuitry stabilizes the kinetochore ensemble to protect CENP-A in the human pathogenic yeast *Candida albicans*. PLoS Genet. **8:**e1002661. doi:10.1371/journal.pgen.1002661.
15. **Tanaka K, Kitamura E, Tanaka TU.** 2010. Live-cell analysis of kinetochore-microtubule interaction in budding yeast. Methods **51:** 206–213.
16. **Asakawa H, Hiraoka Y, Haraguchi T.** 2011. Physical breakdown of the nuclear envelope is not necessary for breaking its barrier function. Nucleus **2:**523–526.
17. **Ding R, McDonald KL, McIntosh JR.** 1993. Three-dimensional reconstruction and analysis of mitotic spindles from the yeast, *Schizosaccharomyces pombe*. J. Cell Biol. **120:**141–151.
18. **Kozubowski L, Heitman J.** 2012. Profiling a killer, the development of *Cryptococcus neoformans*. FEMS Microbiol. Rev. **36:**78–94.
19. **Loftus BJ, Fung E, Roncaglia P, Rowley D, Amedeo P, Bruno D, Vamathevan J, Miranda M, Anderson IJ, Fraser JA, Allen JE, Bosdet IE, Brent MR, Chiu R, Doering TL, Donlin MJ, D'Souza CA, Fox DS, Grinberg V, Fu J, Fukushima M, Haas BJ, Huang JC, Janbon G, Jones SJ, Koo HL, Krzywinski MI, Kwon-Chung JK, Lengeler KB, Maiti R, Marra MA, Marra RE, Mathewson CA, Mitchell TG, Pertea M, Riggs FR, Salzberg SL, Schein JE, Shvartsbeyn A, Shin H, Shumway M, Specht CA, Suh BB, Tenney A, Utterback TR, Wickes BL, Wortman JR, Wye NH, Kronstad JW, Lodge JK, Heitman J, Davis RW, Fraser CM, Hyman RW.** 2005. The genome of the basidiomycetous yeast and human pathogen *Cryptococcus neoformans*. Science **307:**1321–1324.
20. **Kopecká M, Gabriel M, Takeo K, Yamaguchi M, Svoboda A, Ohkusu M, Hata K, Yoshida S.** 2001. Microtubules and actin cytoskeleton in *Cryptococcus neoformans* compared with ascomycetous budding and fission yeasts. Eur. J. Cell Biol. **80:**303–311.
21. **Mochizuki T, Tanaka S, Watanabe S.** 1987. Ultrastructure of the mitotic apparatus in *Cryptococcus neoformans*. J. Med. Vet. Mycol. **25:**223–233.
22. **Straube A, Weber I, Steinberg G.** 2005. A novel mechanism of nuclear envelope break-down in a fungus: nuclear migration strips off the envelope. EMBO J. **24:**1674–1685.
23. **Yamaguchi M, Biswas SK, Ohkusu M, Takeo K.** 2009. Dynamics of the spindle pole body of the pathogenic yeast *Cryptococcus neoformans* examined by freeze-substitution electron microscopy. FEMS Microbiol. Lett. **296:**257–265.
24. **Duan Z, Andronescu M, Schutz K, McIlwain S, Kim YJ, Lee C, Shendure J, Fields S, Blau CA, Noble WS.** 2010. A three-dimensional model of the yeast genome. Nature **465:**363–367.
25. **Roy B, Burrack LS, Lone MA, Berman J, Sanyal K.** 2011. CaMtw1, a member of the evolutionarily conserved Mis12 kinetochore protein family, is required for efficient inner kinetochore assembly in the pathogenic yeast *Candida albicans*. Mol. Microbiol. **80:**14–32.
26. **Sanyal K, Baum M, Carbon J.** 2004. Centromeric DNA sequences in the pathogenic yeast *Candida albicans* are all different and unique. Proc. Natl. Acad. Sci. U. S. A. **101:**11374–11379.
27. **Sanyal K, Carbon J.** 2002. The CENP-A homolog CaCse4p in the pathogenic yeast *Candida albicans* is a centromere protein essential for chromosome transmission. Proc. Natl. Acad. Sci. U. S. A. **99:**12969–12974.
28. **Anderson M, Haase J, Yeh E, Bloom K.** 2009. Function and assembly of DNA looping, clustering, and microtubule attachment complexes within a eukaryotic kinetochore. Mol. Biol. Cell **20:**4131–4139.
29. **Thakur J, Sanyal K.** 2013. Efficient neocentromere formation is suppressed by gene conversion to maintain centromere function at native physical chromosomal loci in Candida *albicans*. Genome Res. **23:** 638–652.
30. **Ohkusu M, Raclavsky V, Takeo K.** 2004. Induced synchrony in *Cryptococcus neoformans* after release from G2-arrest. Antonie Van Leeuwenhoek **85:**37–44.
31. **Richmond D, Rizkallah R, Liang F, Hurt MM, Wang Y.** 2013. Slk19 clusters kinetochores and facilitates chromosome bipolar attachment. Mol. Biol. Cell **24:**566–577.
32. **Wargacki MM, Tay JC, Muller EG, Asbury CL, Davis TN.** 2010. Kip3, the yeast kinesin-8, is required for clustering of kinetochores at metaphase. Cell Cycle **9:**2581–2588.
33. **D'Angelo MA, Hetzer MW.** 2008. Structure, dynamics and function of nuclear pore complexes. Trends Cell Biol. **18:**456–466.
34. **Stavru F, Hülsmann BB, Spang A, Hartmann E, Cordes VC, Görlich D.** 2006. NDC1: a crucial membrane-integral nucleoporin of metazoan nuclear pore complexes. J. Cell Biol. **173:**509–519.
35. **Boehmer T, Enninga J, Dales S, Blobel G, Zhong H.** 2003. Depletion of a single nucleoporin, Nup107, prevents the assembly of a subset of nucleoporins into the nuclear pore complex. Proc. Natl. Acad. Sci. U. S. A. **100:** 981–985.
36. **De Souza CP, Osmani AH, Hashmi SB, Osmani SA.** 2004. Partial nuclear pore complex disassembly during closed mitosis in *Aspergillus nidulans*. Curr. Biol. **14:**1973–1984.
37. **Aoki K, Hayashi H, Furuya K, Sato M, Takagi T, Osumi M, Kimura A, Niki H.** 2011. Breakage of the nuclear envelope by an extending mitotic nucleus occurs during anaphase in *Schizosaccharomyces japonicus*. Genes Cells **16:**911–926.
38. **Yam C, He Y, Zhang D, Chiam KH, Oliferenko S.** 2011. Divergent strategies for controlling the nuclear membrane satisfy geometric constraints during nuclear division. Curr. Biol. **21:**1314–1319.
39. **Theisen U, Straube A, Steinberg G.** 2008. Dynamic rearrangement of nucleoporins during fungal "open" mitosis. Mol. Biol. Cell **19:**1230–1240.
40. **Blower MD, Karpen GH.** 2001. The role of *Drosophila* CID in kinetochore formation, cell-cycle progression and heterochromatin interactions. Nat. Cell Biol. **3:**730–739.
41. **Blower MD, Sullivan BA, Karpen GH.** 2002. Conserved organization of centromeric chromatin in flies and humans. Dev. Cell **2:**319–330.
42. **Moroi Y, Hartman AL, Nakane PK, Tan EM.** 1981. Distribution of kinetochore (centromere) antigen in mammalian cell nuclei. J. Cell Biol. **90:**254–259.
43. **Przewloka MR, Zhang W, Costa P, Archambault V, D'Avino PP, Lilley KS, Laue ED, McAinsh AD, Glover DM.** 2007. Molecular analysis of core kinetochore composition and assembly in *Drosophila melanogaster*. PLoS One **2:**e478. doi:10.1371/journal.pone.0000478.
44. **Kozubowski L, Heitman J.** 2010. Septins enforce morphogenetic events during sexual reproduction and contribute to virulence of *Cryptococcus neoformans*. Mol. Microbiol. **75:**658–675.